Cogn Neurodyn (2015) 9:615–626
DOI 10.1007/s11571-015-9355-z

RESEARCH ARTICLE

A cerebral blood flow evaluation during cognitive tasks following a cervical spinal cord injury: a case study using transcranial Doppler recordings

Héloïse Bleton[1] · **Ervin Sejdić**[1]

Received: 29 January 2015 / Revised: 15 June 2015 / Accepted: 27 August 2015 / Published online: 3 September 2015

Abstract A spinal cord injury (SCI) is one of the most common neurological disorders. In this paper, we examined the consequences of upper SCI in a male participant on the cerebral blood flow velocity. In particular, transcranial Doppler was used to study these effects through middle cerebral arteries (MCA) during resting-state periods and during cognitive challenges (non-verbal word-generation tasks and geometric-rotation tasks). Signal characteristics were analyzed from raw signals and envelope signals (maximum velocity) in the time domain, the frequency domain and the time–frequency domain. The frequency features highlighted an increase of the peak frequency in L-MCA and R-MCA raw signals, which revealed stronger cerebral blood flow during geometric/verbal processes respectively. This underlined a slight dominance of the right hemisphere during word-generation periods and a slight dominance of the left hemisphere during geometric processes. This finding was confirmed by cross-correlation in the time domain and by the entropy rate in information-theoretic domain. A comparison of our results to other neurological disorders (Alzheimer's disease, Parkinson's disease, autism, epilepsy, traumatic brain injury) showed that the SCI had similar effects such as general decreased cerebral blood flow and similar regular hemispheric dominance in a few cases.

Keywords Transcranial Doppler · Spinal cord injury · Cognitive tasks · Cerebral blood flow velocity · Signal processing

✉ Ervin Sejdić
esejdic@ieee.org

[1] Department of Electrical and Computer Engineering, University of Pittsburgh, Pittsburgh, PA 15261, USA

Introduction

Aaslid et al. introduced transcranial Doppler sonography as a non-invasive ultrasonic technique to measure CBFV and its variations. TCD measures activity in the main cerebral arteries through an intact skull (Brass et al. 1988; Aaslid et al. 1982). Some of the advantages of TCD include its high temporal resolution (due to insonation without any interruption; Bernd Ringelstein et al. 1998), its stress-free aspect, and its user-friendliness (Schmidt et al. 1999; Scott Burgin et al. 2000). TCD is typically employed to monitor the cerebral arterial blood flow velocity in major arteries of the circle of Willis (Reid and Spencer 1972; Bishop et al. 1986).

TCD provides information about blood flow modifications due to neural activities in normal and pathological cases (Wong et al. 2000; Zanette et al. 1989; Compton et al. 1987; Markwalder et al. 1984; Krejza et al. 1999). The term "neurovascular coupling" represents the close link which exists between CBFV changes and neural activity (Phillips et al. 2013). Neural activation implies modifications involving cerebral blood perfusion (Fox and Raichle 1986; Deppe et al. 2004). Hence, determining hemisphere dominance during cognitive processes is a typical application of TCD (Deppe et al. 2004; Szirmai et al. 2010; Cupini et al. 1996; Hartje et al. 1994). As the middle cerebral artery (MCA) carries 80 % of cerebral blood to the hemispheres (Lindegaard et al. 1987), the effects of cognitive activities on CBFV in MCAs is usually assessed (Hartje et al. 1994; Droste et al. 1989a; Bulla-Hellwig et al. 1996) using bilateral probes placed on the transtemporal window on both sides of the skull (Larsen et al. 1994; White and Venkatesh 2006). Previous studies have specifically focused on CBFV outcomes during cognitive processes in healthy participants (Kelley et al. 1992;

Vingerhoets and Stroobant 1999). A few studies also highlighted the consequences on cerebral blood flow during resting-state and during mental processes in participants with neurological disorders (e.g., autism, epilepsy, spinal cord injury) (Silvestrini et al. 2006; Knake et al. 2003; Whitehouse and Bishop 2008; Nanda et al. 1974; Curt et al. 2004).

A spinal cord injury (SCI) in patients usually implies partial or full motor/sensory dysfunction (Cirak et al. 2004; Sadowsky et al. 2002), and the severity of SCI is evaluated according to the American Spinal Injury Association Impairment Scale. The majority of previous studies have examined a link between SCIs and CBFV in patients with a high level of SCI, i.e. above the sixth thoracic segment (Phillips et al. 2013; Catz et al. 2007; Houtman et al. 2001). These contributions showed that SCI can lead to other health disorders: cardiovascular and broncho-pulmonary diseases, musculoskeletal, gastro-intestinal, renal and immune dysfunctions in addition to incomplete/complete tetraplegia/paraplegia and dysfunctions (Phillips et al. 2013; Scott et al. 2011). In particular, SCI implies an impairment of supraspinal regulation of autonomic function. This deterioration entails hypotension and sudden peaks of hypertension (Phillips et al. 2013; Krassioukov 2009). An impaired tension control affects the response of cerebral blood flow and brain metabolic demands during mental or physical challenges. In fact, the maintenance of sufficient cerebral blood flow is based on arterial baroreflex and cerebral autoregulation. The cerebral autoregulation adjusts the cerebral blood flow depending on the brain needs while the arterial baroreflex maintains arterial blood pressure. Consequently, the brain response to cognitive processes could be impacted by the dysfunctional tension control, which involves a reduction of focus, memory or reasoning (Morris et al. 1986; Tzeng et al. 2010; Davidoff et al. 1990; Gonzalez et al. 1991). Only a few TCD studies have examined CBFV in SCI patients during mental tasks. These studies show that CBFV through MCA from participants with SCI above the sixth thoracic segment does not increase during cognitive tests (attention and verbal test). This indicates a deficient cognitive performance due to hypotension (Wecht et al. 2012). Nevertheless, CBFV from SCI subjects is constantly lower than CBFV from non-SCI subjects during resting-state periods (Wecht et al. 2012). However, other TCD studies established a clear connection between hypotension and an impaired cerebral blood flow during mental activities (Costa et al. 1998; Duschek and Schandry 2004; Morris et al. 2002). Subjects with hypotension show a reduced CBFV and less distinct CBFV increase during stimulus cognitive activities than the healthy subjects (Duschek et al. 2003).

The current study focused on examining the repercussions of injuries in the upper side of the spinal cord on CBFV. Specifically, we examined CBFV in MCAs during rest periods and cognitive tasks from a male SCI participant on the fifth cervical vertebrae. Our major contributions include the understanding of signal characteristics in the time domain, the frequency domain and the time–frequency domain. We examined both raw signals and the spectral envelope signals, which are peak velocity signals extracted from raw signals (Deppe et al. 1997). These signal characteristics were then compared to CBFV in healthy participants and participants with other neurological disorders.

Methodology

Case study description

This is a case study of CBFV in a single participant with SCI (20 years post the injury). The participant's SCI is at the level of the fifth cervical vertebrae. The subject had no history of heart murmurs, strokes, concussions, migraines or other brain-related injuries. The participant was asked to sign the consent form approved by the University of Pittsburgh Institutional Review Board (Fig. 1).

Data acquisition

The MCA signals were collected with a SONARA TCD System (Carefusion, San Diego, CA, USA). Two 2 MHz transducers were fixed with a headset on both sides of the skull. They were placed on transtemporal windows [5 cm in front of the ears, above the zygomatic arch (Schneider et al. 1988)] to record the MCA signals. MCA were identified depending on the depth of insonation (45–55 mm), the angle of insonation (perpendicularly to the skull) and the flow direction (towards transducers) (White and Venkatesh 2006; Alexandrov et al. 2007). Additionally, the end-tidal carbon dioxide $ETCO_2$ (BCI Capnocheck Sleep Capnograph, Smiths Medical, Waukesha, Wisconsin, USA) was monitored along with respiration rate, electrocardiogram, head movement and skin conductance via a multisystem physiological data monitoring system (Nexus-X, Mindmedia, Netherlands). After

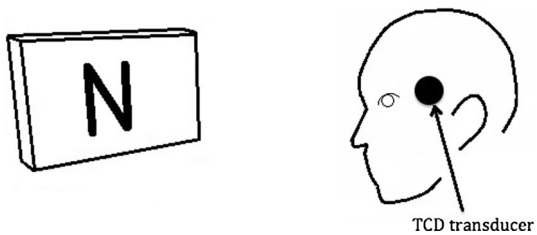

Fig. 1 Setup for the study

the acquisition of R-ACA and L-ACA cerebral blood flow data in the form of audio files, raw signals were extracted with a sampling frequency of 44,100 Hz. Information was downsampled by a factor 5 (8820 Hz) to accelerate computation.

The participant was asked to complete 15 min of resting-state followed by two 15-min periods of cognitive processes. During the 15 min of resting state, the subject was requested to sit motionless and maintain a thought-free mental state. The 15-min periods of mental tasks were separated by a 5-min break. However, we did not collect data during these five minutes. Each 15-min block was comprised of 5 word generation tasks, 5 mental rotation tasks and 5 resting conditions of 45 s between each cognitive task. During geometric tasks, pairs of images were randomly selected from a database constructed from 3-D cubes and were then displayed. Subjects were asked to rotate displayed models to define connections between pairs of images (mirror symmetrical or identical). During the word generation task, letters which were randomly chosen were displayed at the beginning of each period. Participants generated words based on these letters. A non-verbal mode of answering was chosen to avoid activation of brain regions associated with speech. In each mental block, the order of tasks were randomly chosen (Fig. 2).

In this study, raw CBFV signals were collected using TCD. The raw signals are comprised of various velocities of blood particles in cerebral arteries. In fact, signals are composed from several sinusoidal signals due to parabolic speed CBFV distribution (Deppe et al. 2004). We also considered the maximal CBFV or envelope signals, which correspond to the maximal Doppler shift (Deppe et al. 2004; Sejdić et al. 2013).

Feature extraction

Statistical features

MCA signals on the right and the left side were characterized by the second, third, and fourth moments, i.e. standard deviation, skewness, and kurtosis of the signal (Hosking 1990; Papoulis 1991). The standard deviation of the amplitude distribution represents the dispersion of the data from the average of a distribution (Papoulis 1991; Zoubir and Boashash 1998). The skewness of a signal denotes the asymmetry of the distribution (Papoulis 1991; Allen et al. 2004). The kurtosis of a distribution describes the shape of the distribution around the tails (Papoulis 1991; Oja 1990).

The cross-correlation coefficient at the zero lag measures the similarity between two signals (right MCA and left MCA):

$$CC_{X/Y} = \frac{1}{N}\sum_{i=1}^{N}(x_i y_i) \tag{1}$$

where the signals X and Y represent signals from the right and the left side of the MCA (Tiao and Box 1981).

Information-theoretic features

The Lempel–Ziv complexity (LZC) measures the randomness, the predictability, and the regularity of discrete–time signals (Ahmed et al. 2011). It is widely used in biomedical applications, especially to study brain activities (Aboy et al. 2006; Abásolo et al. 2006; Gao et al. 2011). The signal data is transformed into finite sequences. 99 thresholds are defined to divide the signal into 100 finite spaces T_h, $1 \le h \le 99$, $h \in \mathbb{Z}^+$ (Hu et al. 2006). Then, parts of the quantized signal $X_1^n = \{x_1, x_2, \ldots, x_n\}$ are gathered to shape blocks (Lempel and Ziv 1976):

$$B = X_j^l = \{x_j, x_{j+1}, \ldots, x_l\}, \quad 1 \le j \le l \le n, \quad j, l \in Z^+ \tag{2}$$

where each block has the length L defined by $j - l + 1$ and represents a series of successive data. For each L, every block is analyzed. A counter c is defined to illustrate the amount of new pattern formation. c increases by one unit if the sequence of a block has not already appeared in previous analysis. Finally, the LZC was given as the following formula where the final c measures the complexity of the signal and n represents the total of quantized levels in the signal:

$$LZC = \frac{c(log_{100}c + 1)}{n} \tag{3}$$

The entropy rate ρ of a stochastic process measures the statistic degree of the recurrence of patterns of a signal for medical data analysis (Pincus et al. 1991). The normalized pattern distribution (zero mean and unit variance) is quantized into 10 equal levels. Then, the distribution $X = \{x_1, x_2, \ldots, x_n\}$ is decomposed and grouped into blocks of length L, $10 \le L \le 30$. A block L represents a finite sequence of successive samples in a quantized distribution such as $\Omega_L = \{\omega_1, \omega_2, \ldots, \omega_{n-L+1}\}$ (Porta et al. 2011).

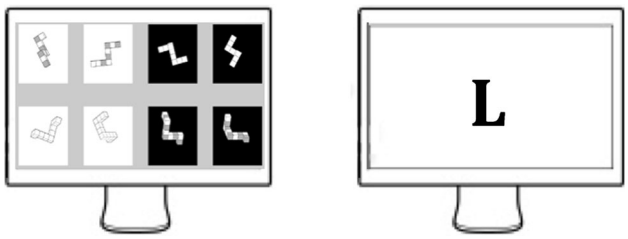

Fig. 2 An on-screen sample of geometric and word-generation tasks

$$\omega_i = 10^{L-1}x_{i+L-1} + 10^{L-2}x_{i+L-2} + \cdots + 10^0 x_i \quad (4)$$

where ω_i is classified between 0 and $10^L - 1$. The Shannon entropy $S(L)$ defines the degree of complexity of ω_L given the quantized signal Ω_L where X takes discrete values ω_j with probability p_j (Porta et al. 2011):

$$S(L) = \sum_{j=0}^{10^{L-1}} p_j \ln p_j \quad (5)$$

where p_j is the approximated sample joint probability of the pattern j in Ω_L with the understanding that $\sum_{j=1}^{n-L+1} p_j = 1$ with $0 \le p_j \le 1 i = 1, \ldots, n-L+1$. The normalized conditional entropy is defined as (Porta et al. 2000):

$$N(L) = \frac{S(L) - S(L-1) + S(1)pe(L)}{S(1)} \quad (6)$$

where $pe(L)$ is the percentage of patterns with length L that appeared only once in ω_L. $S(1)$ is the conditional entropy estimation of the stochastic process for $L = 1$ and represents the Shannon entropy of white noise. It is multiplied by the same probability distribution $pe(L)$. Thus, $S(1)pe(L)$ is a corrective term added due to the underestimation of $S(L) - S(L-1)$ for a larger L (Porta et al. 1998). Given that the first term decreases while the second term increases with L, the function $N(L)$ shows a minimum $min(N(L))$ which is the best estimation of the conditional entropy. $min(N(L))$ is an index of complexity. Conversely, $\rho = 1 - min(N(L))$ is an index of regularity, whose values are between 0 and 1 (Porta et al. 2000).

Two probability functions can be compared thanks to the cross-entropy rate. It quantifies the mutual information between two distributions. It predicts data in a signal from previous and current information in another signal. The two X and Y were normalized, quantized and computed according to the conditional entropy method. Finally, the cross-entropy rate $\Omega_L^{X|Y}$ (information rate available in one of the samples of the quantized signal X when a pattern of $L-1$ samples of the quantized signal Y) is computed as (Porta et al. 2000):

$$\omega_i^{X|Y} = 10^{L-1}x_{i+L-1} + 10^{L-2}y_{i+L-2} + \cdots + 10^0 y_i \quad (7)$$

where $S_X(L)$, $S_Y(L)$ and $S_{X|Y}$ represent the Shannon entropies of the distribution X, Y and $\Omega_L^{X|Y}$. The normalized cross-entropy was established as:

$$NC_{X|Y}(L) = \frac{S_{X|Y}(L) - S_Y(L-1) + S_X(1)pe_{X|Y}(L)}{S_X(1)} \quad (8)$$

where $pe_{X|Y}(L)$ is the percentage of patterns with the length L that appeared only once in $\omega_L^{X|Y}$ and $S_X(1)pe_{X|Y}(L)$ is a corrective term added due to the underestimation of $S_{X|Y}(L) - S_Y(L-1)$ for a larger L. As with the previous method, $S_X(1)$ is the conditional entropy estimation of the stochastic process X for $L = 1$. The Shannon entropy of white noise $S_X(1)$ is multiplied by the same probability distribution $pe_{X|Y}(L)$. The previous function exhibits a minimum $min(NC_{X|Y}(L), NC_{Y|X}(L))$. The index of synchronization $\Lambda_{X|Y} = 1 - min(NC_{X|Y}(L), NC_{Y|X}(L))$ varies between 0 (X and Y are independent processes) and 1 (X and Y are synchronized).

Frequency features

The peak frequency, the centroid frequency, and the bandwidth of the spectrum are examined to identify the spectral characteristics of the signal (Sejdić et al. 2009; Lee et al. 2010; Nishida et al. 2014). The peak frequency is defined as the maximal spectral power:

$$f_p = arg_f max\{|F_X(f)|^2\} \quad (9)$$

where $F_X(f)$ is the Fourier transform of the signal X and f_{max} was 8820 Hz in this study. The spectral centroid is computed as the center of mass of the spectrum (Vergara et al. 2004):

$$f_c = \frac{\int_0^{f_{max}} f|F_X(f)|^2 \, df}{\int_0^{f_{max}} |F_X(f)|^2 \, df} \quad (10)$$

The bandwidth of the spectrum represents the squared differences between the spectral centroid and the spectral components (Sejdić et al. 2009):

$$B = \sqrt{\frac{\int_0^{f_{max}} (f - \widehat{f})^2 |F_X(f)|^2 df}{\int_0^{f_{max}} |F_X(f)|^2 df}} \quad (11)$$

Time–frequency features

Based on a 10-level discrete wavelet decomposition of the signal using the discrete Meyer wavelet, the signal is decomposed into 10 levels $W = [a_{10}d_{10}d_9 \ldots d_1]$ where a_{10} is the approximation coefficient and d_k represents detail coefficient at the kth-level (Hilton 1997). The signal is observed at various frequency bands and various positions. Then, the relative wavelet energy from the approximation coefficients is defined by the following formula (Rosso et al. 2001):

$$\Xi_a = \frac{\|a_{10}\|^2}{\|a_{10}\|^2 + \sum_{k=1}^{10} \|d_k\|^2} (\%) \quad (12)$$

$$\Xi_{d_k} = \frac{\|d_k\|^2}{\|a_{10}\|^2 + \sum_{k=1}^{10} \|d_k\|^2} (\%) \quad (13)$$

where $\|.\|$ is the Euclidian norm. The relative wavelet energy defines the relative energies within different frequency bands depending on ratio between the kth level of decomposition and the total energy of the signal.

A wavelet entropy Ω measures the degree of order/disorder of the signal (Rosso et al. 2001; Han et al. 2013). It represents the concentration of wavelet energies on the band of levels:

$$\Omega = -\Xi_{a_{10}} \log_2 \Xi_{a_{10}} - \sum_{k=1}^{10} \Xi_{d_k} \log_2 \Xi_{d_k} \quad (14)$$

where $\Xi_{a_{10}}$ is the relative energy.

Statistical test

The non-parametric statistical hypothesis Wilcoxon rank-sum test was used to compare statistical differences between results (Bridge and Sawilowsky 1999; DePuy et al. 2005). We examined the effects of the mental task, the geometric task and the resting-state period. $p < 0.05$ indicates the statistical significance of the extracted features (Hayman et al. 1970).

Results

The end-tidal carbon dioxide level does not influence the mean diameter of the middle cerebral arteries (Giller et al. 1993). Consequently, it is not taken into consideration. Secondly, the results are presented in tables in the form of $(mean \pm standard\ deviation)$ where the rest period is pointed out by an "R", the verbal task is indicated by a "V" and a "G" shows the geometric tasks. R-MCA indicates the right MCA, while L-MCA indicates the left MCA.

Time features

Tables 1 and 2 summarize the time-domain feature values for the raw and the envelope signals. For the raw CBFV signals, a few statistical differences were detected. The standard deviation in R-MCA decreased during cognitive tasks ($p < 0.05$), deviation was larger during the geometric tasks than during the word-generation tasks ($p = 0.04$). Furthermore, statistical differences were noticed between resting-state periods and mental processes in the kurtosis value on the left-sided signals ($p < 0.05$). The kurtosis was higher during cognitive challenges than during baseline periods (particularly during word-generation tasks). While considering the features on the envelope signals, a lower correlation value was noticed during verbal tasks than during the resting-state periods ($p = 0.05$).

Table 1 Time features from raw CBFV signals

	Raw	
	R-MCA	L-MCA
Mean CBFV		
R	$(10.7 \pm 6.94)^{b}$	$(-4.45 \pm 3.56)^{b}$
V	$(1.12 \pm 7.00)^{b}$	$(0.18 \pm 6.67)^{b}$
G	$(3.13 \pm 8.18)^{b}$	$(0.89 \pm 6.51)^{b}$
SD		
R	0.14 ± 0.01	0.12 ± 0.01
V	0.10 ± 0.02	0.10 ± 0.02
G	0.12 ± 0.01	0.12 ± 0.01
Skewness		
R	$(-1.11 \pm 0.71)^{a}$	$(-2.03 \pm 4.44)^{a}$
V	$(0.39 \pm 5.51)^{a}$	$(0.52 \pm 6.70)^{a}$
G	$(0.91 \pm 2.87)^{a}$	$(-0.39 \pm 5.60)^{a}$
Kurtosis		
R	3.11 ± 0.04	$3.09 \pm (3.92)^{a}$
V	3.40 ± 0.19	3.37 ± 0.22
G	3.28 ± 0.23	3.28 ± 0.18
Cross-correlation		
R	$(15.0 \pm 1.97)^{a}$	
V	$(13.7 \pm 1.50)^{a}$	
G	$(14.2 \pm 1.89)^{a}$	

CBFV are in units of centimeters per second

[a] Multiplication by 10^{-3}

[b] Multiplication by 10^{-7}

Information-theoretic features

Information-theoretic features from both CBFV raw and CBFV envelope signals are presented in Tables 3 and 4. For the envelope signals, the entropy rate was higher during the geometric-rotation periods in R-MCA than in L-MCA ($p = 0.05$).

Frequency features

Tables 5 and 6 summarize the frequency characteristics of raw and envelope signals. For the raw signals, the peak frequency was higher during geometric-rotation tasks than during verbal processes in L-MCA ($p = 0.05$). Additionally, a statistical difference on the peak frequency was observed between R-MCA and L-MCA during word-generation tasks. The peak frequency of R-MCA was higher ($p = 0.02$). The bandwidth values of R-MCA signals increased during cognitive processes ($p < 0.05$). The bandwidth was larger during verbal tasks than it was during geometric-rotation periods ($p = 0.04$). For the envelope

Table 2 Time features from envelope CBFV signals

	Envelope	
	R-MCA	L-MCA
Mean CBFV		
R	38.0 ± 8.68	36.6 ± 5.41
V	37.2 ± 6.25	36.0 ± 4.96
G	33.0 ± 6.06	33.3 ± 4.79
SD		
R	9.18 ± 2.39	9.89 ± 2.51
V	15.8 ± 4.41	15.0 ± 5.23
G	12.6 ± 3.96	11.3 ± 3.07
Skewness		
R	1.01 ± 0.50	0.96 ± 0.15
V	1.47 ± 0.45	1.40 ± 0.47
G	1.80 ± 0.62	1.60 ± 0.56
Kurtosis		
R	4.76 ± 2.13	4.07 ± 0.59
V	5.84 ± 2.49	5.45 ± 1.86
G	7.76 ± 3.30	6.90 ± 2.71
Cross-correlation		
R	0.97 ± 0.01	
V	0.88 ± 0.06	
G	0.91 ± 0.06	

CBFV are in units of centimeters per second

Table 3 Information-theoretic features from raw CBFV signals

	Raw	
	R-MCA	L-MCA
LZC		
R	0.68 ± 0.01	0.69 ± 0.01
V	0.68 ± 0.02	0.68 ± 0.01
G	0.68 ± 0.02	0.67 ± 0.01
Entropy rate		
R	0.41 ± 0.10	0.34 ± 0.10
V	0.37 ± 0.10	0.41 ± 0.07
G	0.42 ± 0.11	0.44 ± 0.09
Index synchronization		
R	0.35 ± 0.08	
V	0.36 ± 0.08	
G	0.38 ± 0.10	

signals, a small increase of the R-MCA bandwidth was noticed during the verbal processes in comparison to the resting-states ($p = 0.03$). In addition, larger peak frequency in L-MCA signals was observed during geometric-rotation periods than during verbal challenges ($p = 0.01$). A rise of peak frequency was observed on the R-MCA between mental processes (higher during geometric processes than during word-generation tasks). However, the p value is not significant enough on the right side to be considered ($p = 0.2$).

Table 4 Information-theoretic features from envelope CBFV signals

	Envelope	
	R-MCA	L-MCA
LZC		
R	0.66 ± 0.05	0.68 ± 0.04
V	0.66 ± 0.04	0.67 ± 0.03
G	0.63 ± 0.04	0.66 ± 0.04
Entropy rate		
R	0.04 ± 0.03	(3.69 ± 1.62)[a]
V	0.07 ± 0.07	0.04 ± 0.05
G	0.12 ± 0.09	0.06 ± 0.06
Index synchronization		
R	0.12 ± 0.04	
V	0.12 ± 0.06	
G	0.16 ± 0.13	

[a] Multiplication by 10^{-3}

Table 5 Frequency features from raw CBFV signals

	Raw	
	R-MCA	L-MCA
Spectral centroid		
R	897 ± 149	898 ± 108
V	923 ± 104	887 ± 69
G	849 ± 105	842 ± 75
Peak frequency		
R	644 ± 170	600 ± 90.5
V	764 ± 579	446 ± 54.9
G	732 ± 595	884 ± 755
Bandwidth		
R	495 ± 26.7	554 ± 53.5
V	636 ± 65.8	615 ± 80.3
G	579 ± 54.8	565 ± 46.3

Time–frequency features

Tables 7 and 8 shows the wavelet entropy values for the raw and envelope signals. The wavelet entropy values for the raw signals increased during the verbal processes in comparison to other periods on the right side of CBFV signals ($p < 0.05$). Statistical differences between baseline periods and cognitive processes were highlighted on the two sides of CBFV envelope signals ($p < 0.03$). An increase in wavelet entropy was observed on R-MCA and L-MCA signals. Each side of MCA showed an increase of

Table 6 Frequency features from envelope CBFV signals

	Envelope	
	R-MCA	L-MCA
Spectral centroid		
R	8.46 ± 1.84	13.2 ± 3.20
V	15.3 ± 1.77	14.8 ± 2.35
G	13.9 ± 3.25	14.4 ± 1.71
Peak frequency		
R	1.56 ± 0.97	1.76 ± 0.77
V	0.54 ± 0.88	0.62 ± 0.81
G	1.25 ± 1.08	1.84 ± 0.80
Bandwidth		
R	12.1 ± 0.75	13.6 ± 1.17
V	14.4 ± 0.30	14.3 ± 0.50
G	13.8 ± 0.90	14.1 ± 0.38

Table 7 Wavelet entropy values for raw CBFV signals

	Raw	
	R-MCA	L-MCA
Ω		
R	1.60 ± 0.06	1.73 ± 0.10
V	1.81 ± 0.10	1.83 ± 0.12
G	1.71 ± 0.08	1.75 ± 0.07

Table 8 Wavelet entropy values for envelope CBFV signals

	Envelope	
	R-MCA	L-MCA
Ω		
R	0.04 ± (0.54)[a]	0.05 ± (5.68)[a]
V	0.13 ± 0.06	0.13 ± 0.07
G	0.11 ± 0.05	0.10 ± 0.05

[a] Multiplication by 10^{-3}

wavelet energy which was larger during verbal processes than during the other periods.

Figures 3 and 4 present the feature values of wavelet energy decomposition on the raw and the envelope signals. The relative energy of a raw CBFV signal was mainly concentrated in d_{10}, d_9, d_8 and d_7, while the relative energy of the envelope signal was concentrated in a_{10} during all periods. The relative energy of R-MCA raw signals in d_{10} increased during cognitive processes ($p < 0.05$), while diminishing in d_8 during the geometric-rotation processes ($p = 0.03$). The concentration on the level a_{10} from the envelope signals remained relatively stable (with a slight decrease) between the baseline results and cognitive processes on the two sides of MCA ($p = 0.03$).

Discussion

Each domain (time, frequency and time–frequency domains) revealed the effects of cognitive tasks on CBFV in R-MCA and L-MCA, demonstrating the consequences and the repercussions of a spinal cord injury at a cervical level.

The probability density function shapes of R-MCA and L-MCA signals were examined based on the analysis of time domain components. Raw R-MCA signals exhibited small standard deviation values during mental processes, particularly during word-generation periods. This demonstrated that the CBFV signals were more concentrated around the mean of probability density function during the cognitive challenges. In fact, it proved that the cerebral blood flow changed to a larger extent in the case of geometric processes than in the case of word-generation tasks. Changes in kurtosis values for raw L-MCA signals between the resting-state and the cognitive tasks were also noticed. The rise of kurtosis was higher during word-generation tasks than during geometric-rotation challenges. First, it proved that the CBFV variations on the left side of MCA were different depending on the cognitive task type. Second, the kurtosis represented the peakedness and flatness of the distribution (DeCarlo 1997). The higher kurtosis value proved that the cerebral blood flow is massed around one value. Indeed, the left-sided raw signals were more dispersed during the verbal challenges than during the geometric tasks. Signals extracted during the verbal tasks centralized information around one value because of the lower right-sided standard deviation and the higher left-sided kurtosis. During the word-generation periods, cross-correlation of envelope signals decreased compared to the resting-state periods. In fact, a reduction of the cross-correlation values between the verbal tasks and the baseline underlined the lower dependence between right-sided and left-sided signals. This implies a lower dependence on the functioning of the two hemispheres pointing out a lateralization, which implies modifications of the bilateral dependence between the two hemispheres. In this study, the verbal processes may cause a lateralization, where one hemisphere is more engaged in cerebral blood perfusion.

In the information-theoretic domain, the L-MCA envelope signals exhibited lower entropy rates than R-MCA signals during the geometric-rotation tasks, which proved that these signals were more random than right-sided signals. Additionally, a lower entropy highlighted a faster cerebral blood flow. In this way, CBFV was higher

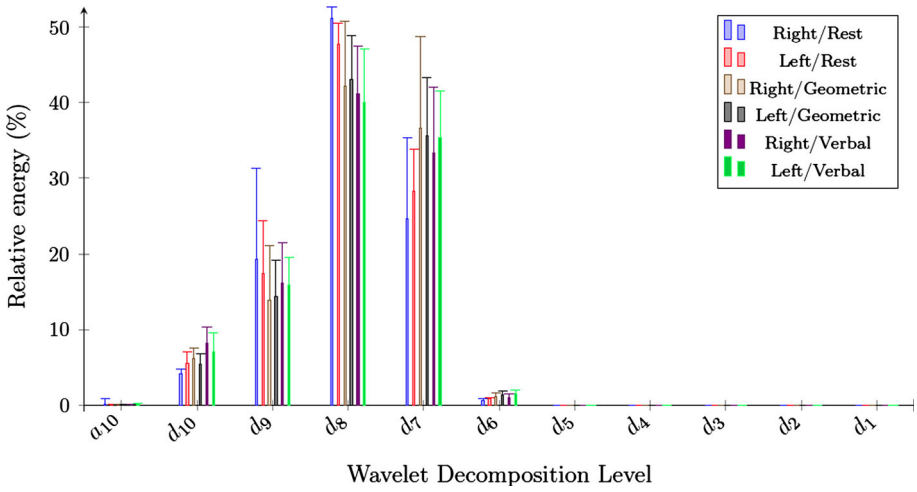

Fig. 3 The 10 level wavelet decomposition of raw signals

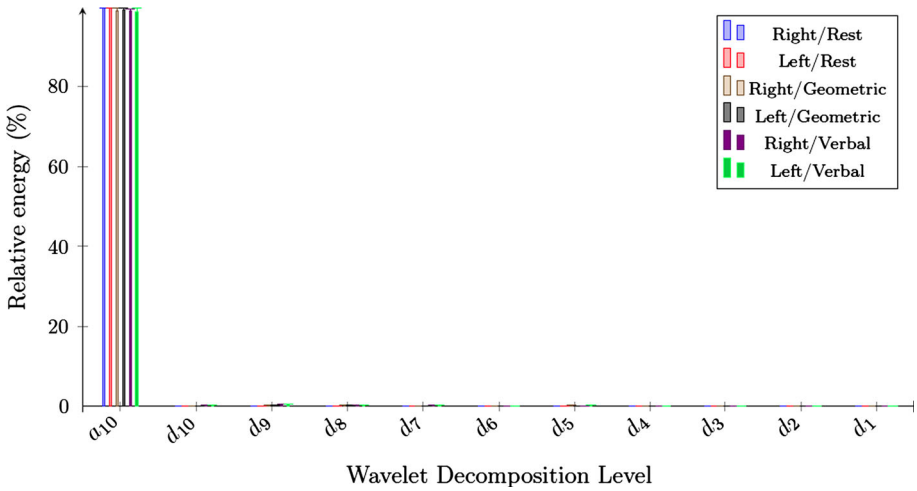

Fig. 4 The 10 level wavelet decomposition of envelope signals

on the left side of MCA during the geometric tasks. Finally, the information-theoretic domain revealed a lateralization during the brain response while performing geometric tasks, where the left brain regions were more activated than the right brain regions.

In the frequency domain, the raw signals showed a band-pass profile, while the envelope outcomes exhibited a low-pass structure. Furthermore, a noticeable increase of the peak frequency in the L-MCA and R-MCA raw signals revealed a stronger cerebral blood flow during the geometric/verbal processes respectively. This increase in peak frequencies denotes a faster variation of cerebral blood flow velocity during the cognitive challenges. It reinforced the previous statements about a left lateralization during the geometric-rotation periods (highlighted by the information-theoretic domain) and a right lateralization during the word-generation tasks (highlighted by the time-domain). Lastly, the bandwidth of R-MCA was larger during the cognitive tasks than during the resting-state, indicating faster cerebral blood flow variations.

Lower wavelet entropy values demonstrated that the raw and envelope signals were more ordered during the rest periods than during the cognitive challenges. In fact, time–frequency domain proved once again that the mental processes led to variations of CBFV signals when compared to the resting state. Furthermore, a very low wavelet entropy implies a very ordered signal, which refers to a periodic mono-frequency signal in the case of envelope signals (Rosso et al. 2001). We noticed statistical differences in the raw and the envelope wavelet energy outcomes. Concerning the raw CBFV signals, a global increase of wavelet energy on d_{10} was noticed in the right side of MCA during the mental challenges when compared to the baseline outcomes. The slight decrease of wavelet energy on a_{10} was also considered on both sides of MCA during the cognitive processes from the envelope results. Modifications of energy distribution were caused by modifications of CBFV during cognitive tasks in the two sides of MCA. However, the wavelet energy did not provide sufficient modifications to observe lateralization during the mental processes.

Finally, a dominance of one hemisphere was concluded during each cognitive task: the preeminence of R-MCA/L-MCA during word-generation periods or geometric-rotation tasks. In fact, the CBFV is higher in one side of the brain than in the other side depending on the type of cognitive process. However, only a few noticeable statistical differences proved to be lateralizations during the mental tasks, leading us to believe that brain lateralization in this patient is not as pronounced.

Next, CBFV from the able-bodied participants and the participant with cervical SCI were compared during each period. CBFV outcomes and brain response from healthy participants were extracted from different studies (Kelley et al. 1992; Vingerhoets and Stroobant 1999; Sejdić et al. 2013; Li et al. 2014). These outcomes pointed out higher mean maximum velocities on MCA from the control subjects (either during the resting-state or during the cognitive challenges). CBFV increased by 37–49 % during each period between able-bodied participants and the SCI participant. A few studies also emphasized a lateralization of CBFV on MCA signals during the mental processes from healthy participants. In fact, the geometric task should lead to a dominance of the left hemisphere (L-MCA), while the word-generation processes should lead to a dominance of the right hemisphere (R-MCA) evidenced by the results from the healthy participants (Hartje et al. 1994; Kelley et al. 1992; Vingerhoets and Stroobant 1999; Droste et al. 1989b). The outcomes from the participant affected by a cervical SCI displayed a similar slight lateralization during the cognitive periods. The participant affected by a cervical SCI presented a "regular" brain lateralization during the cognitive challenges, which was couterbalanced by a low cerebral blood flow. Additionally, a brain functioning difference was observed between the rest and mental processes. A CBFV decrease was discovered in the case of SCI subject, while a CBFV rise was noticed in the case of control subjects during the cognitive periods when compared to the resting-state (Kelley et al. 1992; Vingerhoets and Stroobant 1999).

Lastly, the results from the participant with SCI were compared to the results from subjects affected by other "frequent" neurological disorders, including Alzheimer's disease, autism, epilepsy, Parkinson's disease, and traumatic brain injury (TBI) (Hirtz et al. 2007). Similar to our results, several studies involving Alzheimer's disease, Parkinson's disease (with deficient cognitive response and/or dementia), epileptic and autistic subjects showed a similar deficient brain response to the SCI subject. These brain perfusion responses were characterized by low CBFV (Claassen et al. 2009; Shih et al. 1999; Rombouts et al. 2005; Derejko et al. 2006; Standring 2008; George et al. 1992). Regarding epilepsy, the CBFV decrease was highlighted during abscence attacks (by 70 %) (Fisher et al. 2005; Bode 1992; Diehl et al. 1997; Joo et al. 2008). Nevertheless, only a few studies involving the previous neurological disorders highlighted normal hemisphere functioning during cognitive tasks. Autistic and epileptic subjects may present normal lateralization during cognitive processes (Escalante-Mead et al. 2003; Adcock et al. 2003; Everts et al. 2010; Knecht et al. 1998). On the other hand, the left or right hemisphere is less involved in brain functioning during cognitive tasks than in SCI hemisphere functioning (in the event of Alzheimer's disease, Parkinson's disease, autism in a few cases and epilepsy in a few cases) (Derejko et al. 2006; Tachibana et al. 1993; Burroni et al. 2008; Dawson 1982). Additionally, hypoperfusion is a cause of low CBFV in the case of Alzheimer's disease and Parkinson's disease, since as it is the origin of low CBFV in the case of SCI subjects (Derejko et al. 2006; Tachibana et al. 1993). Finally, similarities and dissimilarities between traumatic brain injury (TBI) and SCI were studied. TBI is deeply related to SCI. A TBI happens in 91 % of traumatic SCI cases (Wecht et al. 2012; Dowler et al. 1995). This implies a decreased cerebral blood flow following the injuries (Soustiel et al. 2005). TBI patients usually present hypotension like SCI subjects (Ghajar 2000; Marmarou et al. 1991). One study revealed normal and abnormal brain lateralization during language tasks in the case of left hemispheric TBI (Rasmussen and Milner 1977).

Conclusion

In this article, we analyzed MCA cerebral blood flow velocity signals from a participant affected by a 5th cervical spinal cord injury during the resting-state, the word-generation tasks and the geometric-rotation tasks. The time-domain, information-theoretic and frequency domains highlighted a right dominance of the MCA during verbal processes and a left dominance of the MCA during geometric processes. The comparison between outcomes from able-bodied subjects and a participant with SCI pointed out a "regular" brain lateralization during cognitive periods and a general decrease of CBFV on the two sides of MCA during each period in the case of SCI. However, higher CBFV was emphasized during rest periods from SCI outcomes, which was the difference between control and SCI subjects. A comparison of SCI to other neurological disorders (Alzheimer's disease, autism, epilepsy, Parkinson's disease, and TBI) underlined common features in a few cases, such as, lower CBFV and normal brain lateralization during mental activities.

References

Aaslid A, Markwalder T, Nornes H (1982) Noninvasive transcranial Doppler ultrasound recording of flow velocity in basal cerebral arteries. J Neurosurg 57(6):769–774

Abásolo D, Hornero R, Gómez C, García M, López M (2006) Analysis of EEG background activity in Alzeimer's disease patients with Lempel–Ziv complexity and central tendency measure. Med Eng Phys 28(4):315–322

Aboy M, Hornero R, Abásolo D, Álvarez D (2006) Interpretation of the Lempel–Ziv complexity measure in the context of biomedical signal analysis. IEEE Trans Biomed Eng 53(11):2282–2288

Adcock J, Wise R, Oxbury J, Matthews P (2003) Quantitative fMRI assessment of the differences in lateralization of language-related brain activation in patients with temporal lobe epilepsy. NeuroImage 18(2):423–438

Ahmed S, Shahjahan M, Murase K (2011) A Lempel–Ziv complexity-based neural network pruning algorithm. Int J Neural Syst 21(5):427–441

Alexandrov A, Sloan M, Wong L, Douville C, Razumovsky A, Koroshetz W, Kaps M, Tegeler C (2007) Practice standards for transcranial Doppler ultrasound: part I—test performance. J Neuroimaging 17(1):11–18

Allen J, Coan J, Nazarian M (2004) Issues and assumptions on the road from raw signals to metrics of frontal EEG assymetry in emotion. Biol Psychol 67(1–2):183–218

Bernd Ringelstein E, Droste D, Babikian V, Evans D, Grosset D, Kaps M, Markus H, Russell D, Siebler M (1998) Consensus on microembolus detection by TCD. Stroke 29(3):725–729

Bishop C, Powell S, Rutt D, Browse N (1986) Transcranial Doppler measurement of middle cerebral artery blood flow velocity: a validation study. Stroke 17(5):913–915

Bode H (1992) Intracranial blood flow velocities during seizures and generalized epileptic discharges. Eur J Pediatr 151(9):706–709

Brass L, Pavlakis S, DeVivo D (1988) Transcranial Doppler measurements of the middle cerebral artery. Effect of hematocrit. Stroke 19(12):1466–1469

Bridge P, Sawilowsky S (1999) Increasing physicians' awareness of the impact of statistics on research outcomes: comparative power of the *t* test and Wilcoxon rank-sum test in small samples applied research. J Clin Epidemiol 52(3):229–235

Bulla-Hellwig M, Vollmer J, Götzen A, Skreczek W, Hartje W (1996) Hemispheric asymmetry of arterial blood flow velocity changes during verbal and visuospatial tasks. Neuropsychologia 34(10):987–991

Burroni L, Orsi A, Monti L, Hayek Y, Rocchi R, Vattimo A (2008) Regional cerebral blood flow in childhood autism: a SPET study with SPM evaluation. Nucl Med Commun 29(2):150–156

Catz A, Bluvshtein V, Korczyn A, Pinhas I, Gelernter I, Nissel T, Vered Y, Bornstein N, Akselrod S (2007) Modified cold pressor test by cold application to the foot after spinal cord injury: suggestion of hemodynamics control by the spinal cord. Am J Phys Med Rehabil 86(11):875–882

Cirak B, Ziegfeld S, Misra Knight V, Chang D, Avellino A, Paidas C (2004) Spinal injuries in children. J Pediatr Surg 39(4):607–612

Claassen J, Diaz-Arrastia R, Martin-Cook K, Levine B, Zhang R (2009) Altered cerebral hemodynamics in early Alzheimer disease: a pilot study using transcranial Doppler. J Alzheimer's Dis 17(3):621–629

Compton J, Redmond S, Symon L (1987) Cerebral blood velocity in subarachnoid haemorrhage: a transcranial Doppler study. J Neurol Neurosurg Psychiatry 50(11):1499–1503

Costa M, Stegagno L, Schandry R, Ricci Bitti P (1998) Contingent negative variation and cognitive performance in hypotension. Psychophysiology 35(6):737–744

Cupini L, Matteis M, Troisi E, Sabbadini M, Bernardi G, Caltagirone C, Silvestrini M (1996) Bilateral simultaneous transcranial Doppler monitoring of flow velocity changes during visuospatial and verbal working memory tasks. Brain 119(4):1249–1253

Curt A, Bruehlmeier M, Leenders K, Roelcke U, Dietz V (2004) Differential effect of spinal cord injury and functional impairment on human brain activation. J Neurotrauma 19(1):43–51

Davidoff G, Roth E, Thomas P, Doljanac R, Dijkers M, Berent S, Morris J, Yarkony G (1990) Depression and neuropsychological test performance in acute spinal cord injury patients: lack of correlation. Arch Clin Neuropsychol 5(1):77–88

Dawson G (1982) Cerebral lateralization in individuals diagnosed as autistic in early childhood. Brain Lang 15(2):353–368

DeCarlo L (1997) On the meaning and use of kurtosis. Psychol Methods 2(3):292–307

Deppe M, Knecht S, Henningsen H, Ringelstein E (1997) Average: a Windows® program for automated analysis of event related cerebral blood flow. J Neurosci Methods 75(2):147–154

Deppe M, Ringelstein E, Knecht S (2004) The investigation of functional brain lateralization by transcranial Doppler sonography. Neuroimage 21(3):1124–1146

DePuy V, Berger V, Zhou Y (2005) Wilcoxon–Mann–Whitney test. Encyclopedia of statistics in behavioral science. Wiley, London

Derejko M, Slawek J, Wieczorek D, Brockhuis B, Dubaniewicz M, Lass P (2006) Regional cerebral blood flow in Parkinson's disease as an indicator of cognitive impairment. Nucl Med Commun 27(12):945–951

Diehl B, Diehl R, Stodieck S, Bernd Ringelstein E (1997) Spontaneous oscillations in cerebral blood flow velocities in middle cerebral arteries in control subjects and patients with epilepsy. Stroke 28(12):2457–2459

Dowler R, O'Brien S, Haaland K, Harrington D, Feel F, Fiedler K (1995) Neuropsychological functioning following a spinal cord injury. Appl Neuropsychol 2(3/4):124–126

Droste D, Harders A, Rastogi E (1989a) A transcranial Doppler study of blood flow velocity in the middle cerebral arteries performed at rest and during mental activities. Stroke 20(8):1005–1011

Droste D, Harders A, Rastogi E (1989b) Two Transcranial Doppler studies on blood flow velocity in both middle cerebral arteries during rest and the performance of cognitive tasks. Neuropsychologia 27(10):1221–1230

Duschek S, Schandry R (2004) Cognitive performance and cerebral blood flow in essential hypotension. Psychophysiology 41(6):905–913

Duschek S, Weisz N, Schandry R (2003) Reduced cognitive performance and prolonged reaction time accompany moderate hypotension. Clin Auton Res 13(6):427–432

Escalante-Mead P, Minshew N, Sweeney J (2003) Abnormal brain lateralization in high-functioning autism. J Autism Dev Disord 33(5):539–543

Everts R, Harvey A, Lillywhite L, Wrennall J, Abbott D, Gonzalez L, Kean M, Jackson G, Anderson V (2010) Language lateralization correlates with verbal memory performance in children with focal epilepsy. Epilepsia 51(4):627–638

Fisher R, Van Emde Boas W, Blume W, Elger C, Genton P, Lee P, Engel J (2005) Epileptic seizures and epilepsy: definitions proposed by the International League Against Epilepsy (ILAE) and the International Bureau for Epilepsy (IBE). Epilepsia 46(4):470–472

Fox P, Raichle M (1986) Focal physiological uncoupling of cerebral blood flow and oxidative metabolism during somatosensory stimulation in human subjects. Proc Natl Acad Sci USA 83(4):1140–1144

Gao J, Hu J, wen Tung W (2011) Complexity measures of brain wave dynamics. Cogn Neurodyn 5(2):171–182

George M, Costa D, Kouris K, Ring H, Ell P (1992) Cerebral blood flow abnormalities in adults with infantile autism. J Nerv Ment Dis 180(7):413–417

Ghajar J (2000) Traumatic brain injury. Lancet 356(9233):923–929

Giller C, Bowman G, Dyer H, Mootz L, Krippner W (1993) Cerebral arterial diameters during changes in blood pressure and carbon dioxide during craniotomy. Neurosurgery 32(5):737–742

Gonzalez F, Chang J, Banovac K, Messina D, Martinez-Arizala A, Kelley R (1991) Autoregulation of cerebral blood flow in patients with orthostatic hypotension after spinal cord injury. Paraplegia 29:1–7

Han C-X, Wang J, Yi G-S, Che Y-Q (2013) Investigation of EEG abnormalities in the early stage of Parkinson's disease. Cogn Neurodyn 7(4):351–359

Hartje W, Ringelstein E, Kistinger B, Fabianek D, Willmes K (1994) Transcranial Doppler ultrasonic assessment of middle cerebral artery blood flow velocity changes during verbal and visuospatial cognitive tasks. Neuropsychologia 32(12):1443–1452

Hayman G, Govindarajulu Z, Leone F, Kim P, Jennrich R (1970) Selected tables in mathematical statistics. American Mathematical Society, Providence

Hilton M (1997) Wavelet and wavelet packet compression of electrocardiograms. IEEE Trans Biomed Eng 44(5):394–402

Hirtz D, Thurman D, Gwinn-Hardy K, Mohamed M, Chaudhuri A, Zalutsky R (2007) How common are the "common" neurologic disorders? Neurology 68(5):326–337

Hosking J (1990) L-moments: analysis and estimation of distributions using linear combinations of order statistics. J R Stat Soc Ser B (Methodol) 52(1):105–124

Houtman S, Serrador J, Colier W, Strijbos D, Shoemaker K, Hopman M (2001) Changes in cerebral oxygenation and blood flow during LBNP in spinal cord-injured individuals. J Appl Physiol 91(5):2199–2204

Hu J, Gao J, Principe J (2006) Analysis of biomedical signals by the Lempel–Ziv complexity: the effect of finite data size. IEEE Trans Biomed Eng 53(12):2606–2609

Joo E, Tae W, Hong S (2008) Cerebral blood flow abnormality in patients with idiopathic generalized epilepsy. J Neurol 255(4):520–525

Kelley R, Chang J, Scheinman N, Levin B, Duncan R, Lee S (1992) Transcranial Doppler assessment of cerebral flow velocity during cognitive tasks. Stroke 23(1):9–14

Knake S, Haag A, Hamer H, Dittmer C, Bien S, Oertel W, Rosenow F (2003) Language lateralization in patients with temporal lobe epilepsy: a comparison of functional transcranial Doppler sonography and the Wada test. NeuroImage 19(3):1228–1232

Knecht S, Deppe M, Ebner A, Henningsen H, Huber T, Jokeit H, Ringelstein E (1998) Noninvasive determination of language lateralization by functional transcranial Doppler sonography. Stroke 29(1):82–86

Krassioukov A (2009) Autonomic function following cervical spinal injury. Respir Physiol Neurobiol 169(2):157–164

Krejza J, Mariak Z, Walecki J, Szydlik P, Lewko J, Ustymowicz A (1999) Transcranial color Doppler sonography of basal cerebral arteries in 182 healthy subjects: age and sex variability and normal reference values for blood flow parameters. J Cereb Blood Flow Metab 172(1):213–218

Larsen F, Olsen K, Hansen B, Paulson O, Knudsen G (1994) Transcranial Doppler is valid for determination of the lower limit of cerebral blood flow autoregulation. Stroke 25(10):1985–1988

Lee J, Sejdić E, Steele C, Chau T (2010) Effects of liquid stimuli on dual-axis swallowing accelerometer signals in a healthy population. Biomed Eng Online 9(1):7

Lempel A, Ziv J (1976) On the complexity of finite sequences. IEEE Trans Inf Theory 22(1):75–81

Li M, Huang H, Boninger M, Sejdić E (2014) An analysis of cerebral blood flow from middle cerebral arteries during cognitive tasks via functional transcranial Doppler recordings. Neurosci Res 84:19–26

Lindegaard K, Lundar T, Wiberg J, Sjøberg D, Aaslid R, Nornes H (1987) Variations in middle cerebral artery blood flow investigated with noninvasive transcranial blood velocity measurements. Stroke 18(6):1025–1030

Markwalder T, Grolimund P, Seiler R, Roth F, Aaslid R (1984) Dependency of blood flow velocity in the middle cerebral artery on end-tidal carbon dioxide partial-pressure. a transcranial ultrasound Doppler study. J Cereb Blood Flow Metab 4(3):368–372

Marmarou A, Anderson R, Ward J, Choi S, Young H, Eisenberg H, Foulkes M, Marshall L, Jane J (1991) Impact of ICP instability and hypotension on outcome in patients with severe head trauma. J Neurosurg 75(1s):S59–S66

Morris J, Roth E, Davidoff G (1986) Mild closed head injury and cognitive deficits in spinal-cord-injured patients: incidence and impact. J Head Trauma Rehabil 1(2):31–42

Morris M, Scherr P, Hebert L, Bennett D, Wilson R, Glynn R, Evans D (2002) Association between blood pressure and cognitive function in a biracial community population of older persons. Neuroepidemiology 21(3):123–130

Nanda R, Wyper D, Harper A, Johnson R (1974) Cerebral blood flow in paraplegia. Paraplegia 12:212–218

Nishida H, Takahashi M, Lauwereyns J (2014) Within-session dynamics of theta–gamma coupling and high-frequency oscillations during spatial alternation in rat hippocampal area CA1. Cogn Neurodyn 7(5):363–372

Oja H (1990) Descriptive statitics for multivariate distributions. Stat Probab Lett 1(6):327–332

Papoulis A (1991) Probability, random variables, and stochastic processes. WCB/McGraw-Hill, New York

Phillips A, Ainslie P, Krassioukov A, Warburton D (2013) Regulation of cerebral blood flow after spinal cord injury. J Neurotrauma 30:1551–1563

Pincus S, Gladstone I, Ehrenkranz R (1991) A regularity statistic fore medical data analysis. J Clin Monit 7(4):335–345

Porta A, Baselli G, Liberati D, Montano N, Cogliati C, Gnecchi-Ruscone T, Malliani A, Cerutti S (1998) Measuring regularity by means of a corrected conditional entropy in sympathetic outflow. Biol Cybern 78(1):71–78

Porta A, Guzzetti S, Montano N, Pagani M, Somers V, Malliani A, Baselli G, Cerutti S (2000) Information domain analysis of cardiovascular variability signals: evaluation of regularity, synchronisation and co-ordination. Med Biol Eng Comput 38(2):180–188

Porta A, Guzzetti S, Montano N, Furlan R, Pagani M, Somers V (2011) Entropy, entropy rate, and pattern classification as tools to typify complexity in short heart period variability series. IEEE Trans Inf Theory 48(11):1282–1291

Rasmussen T, Milner B (1977) The role of early left-brain injury in determining lateralization of cerebral speech functions. Ann NY Acad Sci 299:355–369

Reid J, Spencer M (1972) Ultrasonic Doppler technique for imaging blood vessels. Science 176(4040):1235–1236

Rombouts S, Goekoop R, Stam C, Barkhof F, Scheltens P (2005) Delayed rather than decreased BOLD response as a marker for early Alzheimer's disease. NeuroImage 26(4):1078–1085

Rosso O, Blanco S, Yordanova J, Kolev V, Figliola A, Schrmann M, Basar E (2001) Wavelet entropy: a new tool for analysis of short duration brain electrical signals. J Neurosci Methods 105(1):65–75

Sadowsky C, Volshteyn O, Schultz L, McDonald J (2002) Spinal-cord injury. Disabil Rehabil 24(13):680–687

Schmidt P, Krings T, Willmes K, Roessler F, Reul J, Thron A (1999) Determination of cognitive hemispheric lateralization by "functional" Transcranial Doppler cross-validated by functional MRI. Stroke 30(5):939–945

Schneider P, Rossman M, Bernstein E, Torem S, Ringelstein E, Otis S (1988) Effect of internal carotid artery occlusion on intracranial hemodynamics. Transcranial Doppler evaluation and clinical correlation. Stroke 19(5):589–593

Scott J, Warburton D, Williams D, Whelan S, Krassioukov A (2011) Challenges, concerns and common problems: physiological consequences of spinal cord injury and microgravity. Spinal Cord 49(1):4–16

Scott Burgin W, Malkoff M, Felberg R, Demchuk A, Christou I, Grotta J, Alexandrov A (2000) Transcranial Doppler ultrasound criteria for recanalization after thrombolysis for middle cerebral artery stroke. Stroke 31(5):1128–1132

Sejdić E, Djurović I, Jiang J (2009) Time-frequency feature representation using energy concentration: an overview of recent advances. Digit Signal Proc 19(1):153–183

Sejdić E, Kalika D, Czarnek N (2013) An analysis of resting-state functional transcranial Doppler recordings from middle cerebral arteries. PLoS One 8(2):e55405-1–e55405-9

Shih W, Ashford J, Coupal J, Ryo Y, Stipp V, Magoun S, Gross K (1999) Consecutive brain SPECT surface three-dimensional displays show progression of cerebral cortical abnormalities in Alzheimer's disease. Clin Nucl Med 24(10):773

Silvestrini M, Pasqualetti P, Baruffaldi R, Bartolini M, Handouk Y, Matteis M, Moffa F, Provinciali L, Vernieri F (2006) Cerebrovascular reactivity ad cognitive decline in patients with Alzheimer disease. Stroke 37(4):1010–1015

Soustiel J, Glenn T, Shik V, Boscardin J, Mahamid E, Zaaroor M (2005) Monitoring of cerebral blood flow and metabolism in traumatic brain injury. J Neurotrauma 22(9):955–965

Standring S (2008) Gray's Anatomy: the anatomical basis of clinical practice. Churchill Livingstone, London

Szirmai I, Amrein I, Pálvölgyi L, Debreczeni R, Kamondi A (2010) Evaluation of cerebrovascular spasm with transcranial Doppler ultrasound. J Neurosurg 112(2):37–41

Tachibana H, Kawabata K, Tomino Y, Sugita M, Fukuchi M (1993) Brain perfusion imaging in Parkinson's disease and Alzheimer's disease demonstrated by three-dimensional surface display with ^{123}I-Iodoamphetamine. Dement Geriatr Cogn Disord 4(6):334–341

Tiao G, Box G (1981) Modeling multiple time series with applications. J Am Stat Assoc 76(376):802–816

Tzeng Y, Lucas S, Atkinson G, Willie C, Ainslie P (2010) Fundamental relationships between arterial baroflex sensitivity and dynamic cerebral autoregulation in humans. J Appl Physiol 108(5):1162–1168

Vergara L, Gosalbéz J, Fuente J, Miralles R, Bosch I (2004) Measurement of cement porosity by centroid frequency profiles of ultrasonic grain noise. Biomed Eng Online 84(12):2315–2324

Vingerhoets G, Stroobant N (1999) Lateralization of cerebral blood flow velocity changes during cognitive task: a simultaneous bilateral transcranial Doppler study. Stroke 30(10):2152–2158

Wecht J, Rosado-Rivera D, Jegede A, Cirnigliaro C, Jensen M, Kirshblum S, Bauman W (2012) Systemic and cerebral hemodynamics during cognitive testing. Clin Auton Res 22(1):25–33

White H, Venkatesh B (2006) Applications of transcranial Doppler in the ICU: a review. Intensive Care Med 32(7):981–994

Whitehouse A, Bishop D (2008) Cerebral dominance for language function in adults with specific language impairment or autism. Brain 131(12):3193–3200

Wong K, Li H, Chan Y, Ahuja A, Lam W, Wong A, Kay R (2000) Use of transcranial Doppler ultrasound to predict outcome in patients with intracranial large-artery occlusive disease. Stroke 31(11):2641–2647

Zanette E, Fieschi C, Bozzao L, Roberti C, Toni D, Argentino C, Lenzi G (1989) Comparison of cerebral angiography and transcranial Doppler sonography in acute stroke. Stroke 20(7):899–903

Zoubir A, Boashash B (1998) The bootstrap and its application in signal processing. IEEE Signal Process Mag 15(1):56–76